Operational Strategies for Serving the Multi-Energy Demand

# Operational Strategies for Serving the Multi-Energy Demand

Cristian Piran
*Dipartimento Energia "G. Ferraris"*
*Politecnico di Torino*
Torino, Italy
cristian.piran@studenti.polito.it

Andrea Mazza
*Dipartimento Energia "G. Ferraris"*
*Politecnico di Torino*
Torino, Italy
andrea.mazza@polito.it

Gianfranco Chicco
*Dipartimento Energia "G. Ferraris"*
*Politecnico di Torino*
Torino, Italy
gianfranco.chicco@polito.it

***Abstract*—Multi-energy systems (MES) enable the integration of different energy vectors for serving a multi-energy demand variable in time. MES operation is constrained by different kinds of limits, including limits on the components and limits due to the topology of the interconnections and technical aspects concerning the interactions among MES components. This paper presents a novel extension of the optimization model with linear constraints used in the literature to solve the MES optimization with constant efficiencies and coefficients of performance (*COP*) of the equipment. The extended optimization model considers non-linear convex expressions of the equipment efficiencies and *COP*s and solves the optimization model with linear constraints in an iterative way, until the solution does not change more than a specified tolerance. The optimal MES solutions are shown considering the operation of a trigeneration system that serves electricity, heat and cooling loads in winter and summer cases with specific demand and energy prices, comparing the solutions with constant and variable efficiencies and *COP*.**

***Keywords—Multi-energy system, Operation, Optimization, Efficiency, Energy hub.***

## I. Introduction

In the current trend of energy transition, the deployment of multi-energy systems (MES) [1] provides viable options for the integrated use of different energy vectors in various applications in the industry, the tertiary sector, energy districts, and the evolving energy communities [2].

The MES modelling is effectively formulated by following the energy hub framework [3], in which input-output relations are defined for each MES component, and a matrix-based model is established both for each component and for the entire MES. The energy hub model considers the vector of inputs $\boldsymbol{v_{in}}$, the vector of outputs $\boldsymbol{v_{out}}$, and the coupling matrix $\boldsymbol{C_{out,in}}$, such that:

$$\mathbf{v}_{\text{out}} = \mathbf{C}_{\text{out,in}} \cdot \mathbf{v}_{\text{in}} \quad (1)$$

In the definition of the coupling matrix, if the output from a MES component goes to multiple destinations, specific dispatch factors are defined to represent the share of the output that goes to each destination. The coupling matrix contains both information on the MES topology and the performance of the MES components. The performance is expressed by the efficiencies or the Coefficient of Performance (*COP*) of the equipment. The dispatch factors may be taken as degrees of freedom to be used as decision variables in an optimization procedure referring to a given objective function.

The coupling matrix may be constructed by visual inspection of the MES structure. However, for easier construction, an automatic procedure has been established in [4], considering the energy hub model with dispatch factors. Successively, in [5] it has been discussed that the use of dispatch factors makes the formulation of the constraints for the optimization problem non-linear, because of the products that appear between the decision variables, and a different partitioning of the system variables was proposed, such that the constraints are expressed with a linear formulation, provided that the efficiencies and *COP*s of the equipment are constant (typically equal to their values in rated conditions, i.e., evaluated at full loading). On these bases, the automatic method for constructing the coupling matrix presented in [6] does not use the dispatch factors and uses constant efficiencies and *COP*s as well.

Further evolutions have addressed the use of variable energy efficiencies, transforming the non-linear constraints into linear segments with piecewise linear approximations, as in [7] and [8]. In the mathematical description of the segments, a set of secondary variables is needed to represent the related variables, and further binary values are introduced for guaranteeing the continuity of the segments. The number of segments can be chosen by considering the type of non-linearity of the curve to be linearized.

The piecewise linear approximation can provide a relatively good representation of the non-linear efficiency and *COP* characteristics, at the expense of increasing the number of variables of the model. However, for the equipment considered in a MES, the individual non-linear efficiency and *COP* curves are generally smooth and convex. On these bases, the MES representation used in the energy hub model can be formulated by keeping the efficiency and *COP* curves in their non-linear form, by constructing an iterative procedure to solve the MES optimization, which iterates the solution of the optimization model with linear constraints formulated in [5] by changing at each iteration the numerical values of the efficiencies and *COP*s. The development of such iterative procedure is carried out in this paper, resulting in a novel formulation that does not need the construction of piecewise linear approximations.

The specific novelties of this paper are as follows:

- The formulation and solution of the MES optimization including variable efficiencies and *COP*s defined at variable loading level of the equipment, as an extension of the optimization model with linear constraints from [5].
- The assessment of the performance of the proposed optimization method for solving the MES operation at multiple time steps, compared with the case with constant efficiencies and *COP*s.

The next sections of the paper are organized as follows. Section II recalls the energy hub model in the formulation used to define the optimization model with linear constraints for constant efficiencies and *COP*s, identifying the types of variables used and the corresponding matrix formulation. A

978-1-6654-0557-7/22/$31.00 ©2022 IEEE

worked example is used to show the modelling details. Section III describes the proposed optimization procedure that takes into account non-linear efficiencies and *COP*s. Section IV shows the application of the optimization procedure to representative cases in a trigeneration system that serves electricity, heat and cooling demand. The last section contains the conclusions.

## II. Matrix Modelling of Multi-Energy Systems

### A. Energy hub model - Worked example

In the basic energy hub model, the multi-energy demand (e.g., $W_0$ for electricity, $Q_0$ for heat, and $R_0$ for cooling in Fig. 1) is assumed to be known, with specified demand patterns in a given time period, represented by either the sequence of average power values in each time step inside the period, or by the sequence of energy values. The presence of multiple equipment enables the definition of multiple ways to serve the multi-energy demand with different inputs from the Electricity Distribution System (EDS) and the Fuel Distribution System (FDS), with different multi-energy flows consistent with the technical characteristics of the equipment and with the topology of the interconnections.

The scheme reported in Fig. 1 is used in this paper to construct some worked examples, without loss of generality for the concepts addressed. The following equipment is considered:

- The combined heat and power (CHP) unit, with fuel input $F_{\mathrm{CHP}}$ and simultaneous output of electricity $W_{\mathrm{CHP}}$ and heat $Q_{\mathrm{CHP}}$. The CHP electrical rating $W_{\mathrm{CHP}}^{(\mathrm{ref})}$ and thermal rating $Q_{\mathrm{CHP}}^{(\mathrm{ref})}$ are used as the CHP references. In the input-output energy hub model, the CHP is characterized by the electrical efficiency $\eta_{W,\mathrm{CHP}} = W_{\mathrm{CHP}}/F_{\mathrm{CHP}}$ and thermal efficiency $\eta_{Q,\mathrm{CHP}} = Q_{\mathrm{CHP}}/F_{\mathrm{CHP}}$.
- The auxiliary boiler AB, which serves as a heat backup if the CHP is switched off or the heat demand at the thermal side of the CHP exceeds the thermal rating $Q_{\mathrm{CHP}}^{(\mathrm{ref})}$.
- The electric heat pump EHP, which can supply either the heat or the cooling output (in different operating modes), whose coefficient of performance is $COP_{Q,\mathrm{EHP}} = Q_{\mathrm{EHP}}/W_{\mathrm{EHP}}$ in heating mode and $COP_{R,\mathrm{EHP}} = R_{\mathrm{EHP}}/W_{\mathrm{EHP}}$ in cooling mode.
- The water absorption refrigerator group (WARG), which converts heat into cooling, with coefficient of performance $COP_{\mathrm{WARG}} = R_{\mathrm{WARG}}/Q_{\mathrm{WARG}}$.

### B. Types of variables

To build the linearized model, the variables that appear in the multi-energy scheme for representing the energy flows are partitioned in the following vectors:

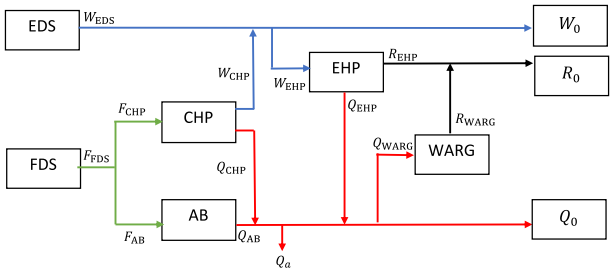


Fig. 1. Scheme of the multi-energy system considered.

a) *output* variables:

$$\mathbf{v}_{\mathrm{out}} = [W_0, \quad Q_0, \quad R_0]^{\mathrm{T}} \tag{2}$$

b) *input* variables:

$$\mathbf{v}_{\mathrm{in}} = [F_{\mathrm{FDS}}, \quad W_{\mathrm{EDS}}]^{\mathrm{T}} \tag{3}$$

c) *intermediate* variables, which include the outputs from every equipment (for the EHP, the variables $Q_{\mathrm{EHP}}$ or $R_{\mathrm{EHP}}$ could be used in alternative, when the EHP operates in heating mode or cooling mode, respectively):

$$\mathbf{v}_{\mathrm{imd}} = [W_{\mathrm{CHP}}, \quad Q_{\mathrm{CHP}}, \quad Q_{\mathrm{AB}}, \quad R_{\mathrm{EHP}}, \quad Q_{\mathrm{EHP}}, \quad R_{\mathrm{WARG}}]^{\mathrm{T}} \tag{4}$$

d) *augmented* variables, which in each bifurcation with $n$ branches represent ($n$-1) degrees of freedom involved; a bifurcation occurs when two or more paths are originated by the same energy vector; from Fig. 1, this happens for the fuel, where the total fuel $F_{\mathrm{FDS}}$ bifurcates into $F_{\mathrm{CHP}}$ and $F_{AB}$, for electricity, where there is the bifurcation into $W_{\mathrm{EHP}}$ and $W_0$, and for heat, in the bifurcation into $Q_{\mathrm{WARG}}$ and $Q_0$, as well as in the bifurcation in which the part $Q_a$ of the heat can be wasted to the ambient and the remaining heat goes forward:

$$\mathbf{v}_{\mathrm{aug}} = [F_{\mathrm{CHP}}, \quad W_{\mathrm{EHP}}, \quad Q_{\mathrm{WARG}}, \quad Q_{\mathrm{a}}]^{\mathrm{T}} \tag{5}$$

The contents of the vector $\mathbf{x} = \left[\mathbf{v}_{\mathrm{in}}^{\mathrm{T}}, \mathbf{v}_{\mathrm{aug}}^{\mathrm{T}}\right]^{\mathrm{T}}$ are not known and are the decision variables of the problem.

The contents of the output vector $\mathbf{v}_{\mathrm{out}}$ are known and in this formulation do not depend on the multi-energy variables or parameters. Hence, these components remain constant, in such a way that the operation of the multi-energy system can be optimized without changing the user's multi-energy demand.

The contents of the intermediate vector $\mathbf{v}_{\mathrm{imd}}$ are not known; however, these contents represent output values that are bounded by the reference (rated) values of the equipment, that is:

$$\mathbf{v}_{\mathrm{imd}}^{(\mathrm{ref})} = \left[W_{\mathrm{CHP}}^{(\mathrm{ref})}, Q_{\mathrm{CHP}}^{(\mathrm{ref})}, Q_{\mathrm{AB}}^{(\mathrm{ref})}, R_{\mathrm{EHP}}^{(\mathrm{ref})}, Q_{\mathrm{EHP}}^{(\mathrm{ref})}, R_{\mathrm{WARG}}^{(\mathrm{ref})}\right]^{\mathrm{T}} \tag{6}$$

### C. Coupling matrix

The energy balances of the three energy vectors can be written by visual inspection, as follows:

*a)* For electricity:

$$W_{\mathrm{EDS}} + \eta_{W,\mathrm{CHP}} \cdot F_{\mathrm{CHP}} - W_{\mathrm{EHP}} - W_0 = 0 \tag{7}$$

*b)* For heat:

$$\eta_{W,\mathrm{CHP}} \cdot F_{\mathrm{CHP}} + \eta_{AB} \cdot (F_{\mathrm{FDS}} - F_{\mathrm{CHP}}) + \\ + COP_{Q,\mathrm{EHP}} \cdot W_{\mathrm{EHP}} + -Q_{\mathrm{WARG}} - Q_0 = 0 \tag{8}$$

*c)* For cooling:

$$COP_{R,\mathrm{EHP}} \cdot W_{\mathrm{EHP}} + COP_{\mathrm{WARG}} \cdot Q_{\mathrm{WARG}} - R_0 = 0 \tag{9}$$

The matrix equation of the system is written in a compact form as in [5]:

$$\begin{vmatrix} \mathbf{v}_{\mathrm{out}} \\ \mathbf{v}_{\mathrm{imd}} \end{vmatrix} = \begin{vmatrix} \mathbf{C}_{\mathrm{out,in}} & \mathbf{C}_{\mathrm{out,aug}} \\ \mathbf{C}_{\mathrm{imd,in}} & \mathbf{C}_{\mathrm{imd,aug}} \end{vmatrix} \begin{vmatrix} \mathbf{v}_{\mathrm{in}} \\ \mathbf{v}_{\mathrm{aug}} \end{vmatrix} = \mathbf{C} \begin{vmatrix} \mathbf{v}_{\mathrm{in}} \\ \mathbf{v}_{\mathrm{aug}} \end{vmatrix} \tag{10}$$

where $\mathbf{C}_{\mathrm{out,in}}$ is the classical coupling matrix used in the energy hub model [3], and $\mathbf{C}$ is the augmented coupling

matrix [5]. The entries of these matrices combine information on the efficiency and *COP* of the equipment with the topology of the interconnections inside the system.

For the worked example, the augmented coupling matrix is written as follows:

$$\mathbf{C} = \begin{bmatrix} 0 & 1 & \eta_{W,\mathrm{CHP}} & -1 & 0 & 0 \\ \eta_{\mathrm{AB}} & 0 & \eta_{Q,\mathrm{CHP}} - \eta_{\mathrm{AB}} & COP_{Q,\mathrm{EHP}} & -1 & -1 \\ 0 & 0 & 0 & COP_{R,\mathrm{EHP}} & COP_{\mathrm{WARG}} & 0 \\ 0 & 0 & \eta_{W,\mathrm{CHP}} & 0 & 0 & 0 \\ 0 & 0 & \eta_{Q,\mathrm{CHP}} & 0 & 0 & 0 \\ \eta_{\mathrm{AB}} & 0 & -\eta_{\mathrm{AB}} & 0 & 0 & 0 \\ 0 & 0 & 0 & COP_{R,\mathrm{EHP}} & 0 & 0 \\ 0 & 0 & 0 & COP_{Q,\mathrm{EHP}} & 0 & 0 \\ 0 & 0 & 0 & 0 & COP_{\mathrm{WARG}} & 0 \end{bmatrix} \tag{11}$$

The first three rows of the matrix **C** contain the coefficients of the energy balances (7)–(9). The other rows contain the coefficients of the output-to-input relations for the individual equipment.

### *C. Optimization model with linear constraints*

If all efficiencies and *COP*s are constant, considering an objective function $f(\mathbf{x})$, e.g., to minimize, it is possible to construct an optimization model with linear constraints, which uses the sub-matrices of the matrix **C** as coefficients, as follows:

$$\min_{\mathbf{x}}\{f(\mathbf{x})\} \tag{12}$$

$$\text{s.t.} \quad \mathbf{v}_{\mathrm{out}} - |\mathbf{C}_{\mathrm{out},in} \ \mathbf{C}_{\mathrm{out},aug}|\,\mathbf{x} = \mathbf{0}$$
$$\mathbf{v}_{\mathrm{imd}}^{(\mathrm{ref})} - |\mathbf{C}_{\mathrm{imd},in} \ \mathbf{C}_{\mathrm{imd},aug}|\,\mathbf{x} \geq \mathbf{0}$$

The objective function can be for example the minimum operation cost, formulated taking into account the fuel price $\rho_F$, the price $\rho_{W,\mathrm{buy}}$ of the electricity bought from the EDS, and the price $\rho_{W,\mathrm{sell}}$ of the electricity sold to the EDS, as:

$$f(\mathbf{x}) = \rho_F \cdot F_{\mathrm{FDS}} + \rho_{W,\mathrm{buy}} \cdot \max\{W_{\mathrm{EDS}}, 0\} + \\ + \rho_{W,\mathrm{sell}} \cdot \min\{W_{\mathrm{EDS}}, 0\} \tag{13}$$

Additional constraints can be included, such as the minimum technical limit of the CHP, below which the CHP is switched off. In this case, the domain of definition of the CHP operation would become discontinuous. However, the discontinuity can be handled by introducing a binary variable $u$, writing the CHP limits $(W_{CHP}^{(\min)}, W_{CHP}^{(\mathrm{ref})})$ on the electrical output as $W_{\mathrm{CHP}}^{(\min)} u \leq W_{\mathrm{CHP}} \leq W_{\mathrm{CHP}}^{(\mathrm{ref})} u$ [11]. Then, the two inequalities can be partitioned as $W_{\mathrm{CHP}} \geq W_{\mathrm{CHP}}^{(\min)} u$, and $-W_{\mathrm{CHP}} \geq -W_{\mathrm{CHP}}^{(\mathrm{ref})} u$. The limits on the CHP thermal output can be handled in a similar way.

This optimization problem can be solved with a standard solver that handles linear constraints.

## III. Extension of the Optimization Model to Consider Non-Constant Efficiencies and *COP*s

### *A. Non-constant efficiencies*

The optimization model with linear constraints provides the optimal solution in a simple way when the efficiencies and *COP*s are constant. However, the hypothesis of constant efficiencies and *COP*s is generally too limiting to characterize the input-output performance of the multi-energy system in a practically meaningful way.

Considering the typical efficiency curves of the components, drawn from experimental results available in the literature and synthesized in [12], it can be seen that:

*a)* For the AB, an expression that represents the AB efficiency $\eta_{AB}$ in terms of the heat output $Q_{AB}$, the heat output level $q_{AB} = Q_{AB}/Q_{AB}^{(ref)}$, the AB losses $Q_{AB}^{(losses)}$, and the relative AB losses $q_{AB}^{(losses)} = Q_{AB}^{(losses)}/Q_{AB}^{(ref)}$ is:

$$\eta_{\mathrm{AB}} = \frac{q_{\mathrm{AB}}}{q_{\mathrm{AB}} + q_{\mathrm{AB}}^{(\mathrm{losses})}} \tag{14}$$

where the relative AB losses $Q_{\mathrm{AB}}^{(\mathrm{losses})}$ can be written in a polynomial form, considering the curve-fitting coefficients $\upsilon_0$, $\upsilon_1$ and $\upsilon_2$:

$$q_{\mathrm{AB}}^{(\mathrm{losses})} = \upsilon_0 + \upsilon_1 \cdot q_{\mathrm{AB}} + \upsilon_2 \cdot q_{\mathrm{AB}}^2 \tag{15}$$

*b)* For the CHP, the partial-load electrical and thermal efficiencies ( $\eta_{W,CHP}$ and $\eta_{Q,CHP}$, respectively) can be approximated in a linear way, or with a second-order model in the region of CHP operation (from the minimum technical limit to the rated conditions):

$$\eta_{W,\mathrm{CHP}} = c_{W,0} + c_{W,1} \cdot W_{\mathrm{CHP}} + c_{W,2} \cdot W_{\mathrm{CHP}}^2 \tag{16}$$

$$\eta_{Q,\mathrm{CHP}} = c_{Q,0} + c_{Q,1} \cdot Q_{\mathrm{CHP}} + c_{Q,2} \cdot Q_{\mathrm{CHP}}^2 \tag{17}$$

where the terms $c_{W,0}$, $c_{W,1}$, $c_{W,2}$, $c_{Q,0}$, $c_{Q,1}$, and $c_{Q,2}$ are curve-fitting coefficients.

### *B. Non-constant COP*

For the WARG, based on the typical partial-load performance, the *COP* variation with respect to the cooling output $R_{\mathrm{WARG}}$ and cooling output level $r_{\mathrm{WARG}} = R_{\mathrm{WARG}}/R_{\mathrm{WARG}}^{(\mathrm{ref})}$ can be expressed as

$$COP_{\mathrm{WARG}} = \frac{r_{\mathrm{WARG}}}{r_{\mathrm{WARG}} + \varsigma_0 + \varsigma_1 \cdot r_{\mathrm{WARG}} + \varsigma_2 \cdot r_{\mathrm{WARG}}^2} \tag{18}$$

where $\varsigma_0$, $\varsigma_1$ and $\varsigma_2$ are curve-fitting coefficients.

For the EHP, the main dependence of the *COP* is on temperature. Therefore, at a given temperature level, for the application presented in this paper the *COP* is considered constant.

### *C. Computational aspects*

A significant practical aspect is that, as seen in the previous section, the efficiencies and *COP*s at partial load are generally linear (thus convex), or non-linear and convex. Based on this consideration, in this paper the use of the linear optimization procedure [5] is extended to the case with non-constant efficiencies and *COP*s by creating an iterative procedure that updates the parameters until an effective optimal solution is found (Fig. 2).

Under the above assumptions, the variables and parameters of the optimization procedure are identified as follows:

$\mathbf{x} = [F_{\mathrm{FDS}}, W_{\mathrm{EDS}}, F_{\mathrm{CHP}}, W_{\mathrm{EHP}}, Q_{\mathrm{WARG}}, Q_{\mathrm{a}}]^{\mathrm{T}}$, vector of the optimization variables; and,

$\boldsymbol{\xi} = \left[\eta_{\mathrm{AB}}, \eta_{e,\mathrm{CHP}}, \eta_{\mathrm{t,CHP}}, COP_{\mathrm{WARG}}\right]^{\mathrm{T}}$, vector of the variable parameters (efficiencies and *COP*). The EHP parameter is considered constant in this example.

The main steps of the overall optimization procedure (summarised in Fig. 2) are:

a) *Initial optimal solution*: the optimization (12) of the multi-energy system operation is solved with constant efficiencies and *COP*s, equal to the rated values, obtaining the output variables.
b) *Efficiency and COP update*: calculation of the new efficiencies and *COP*s from the equations indicated in Section III.A and Section III.B, respectively.
c) *Iterative re-optimization*: the optimization (12) is executed again with the updated efficiencies and *COP*s; the steps b) and c) are repeated until the stop criterion is satisfied.
d) *Stop criterion*: the procedure stops when the maximum variation of the variables in two successive iterations is lower than the predefined tolerance $\varepsilon$.

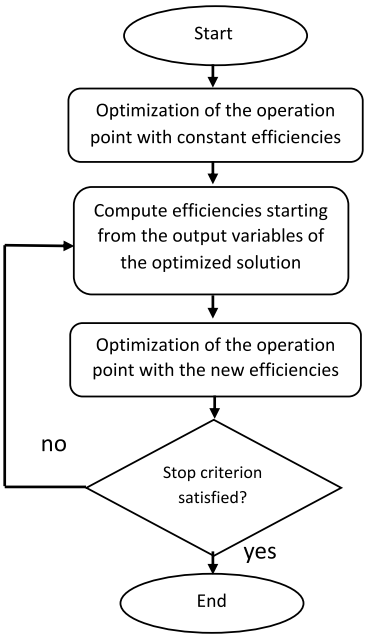


Fig. 2. Flow-chart of the procedure to carry out the optimization with non-constant efficiencies.

Concerning the computational burden, the computation time ratio $\tau_r$ is defined as the ratio between the computation time with variable efficiency and the computation time with constant efficiency. Moreover, the average computation time per iteration $\tau_a$ is also considered in the cases with variable efficiency.

## IV. Application to Representative Cases

### A. Multi-Energy System Data

The case study presented in this paper considers the multi-energy scheme shown in Fig. 1. The rated values of the equipment used (size and efficiency or *COP*) are indicated in Table I. For each equipment represented with non-constant efficiencies or *COP*, Fig. 3 shows the variability of the related parameter in function of the loading level. The curve-fitting coefficients used are indicated in Table II.

Table I. Rated Values for the Equipment Considered

| | ***W*,CHP** | ***Q*,CHP** | **AB** | **WARG** | ***Q*,EHP** | ***R*,EHP** |
|---|---|---|---|---|---|---|
| **size [kW]** | 300 | 450 | 800 | 400 | 400 | 400 |
| **efficiency or *COP*** | 0.3 | 0.45 | 0.85 | 0.65 | 3 | 3 |

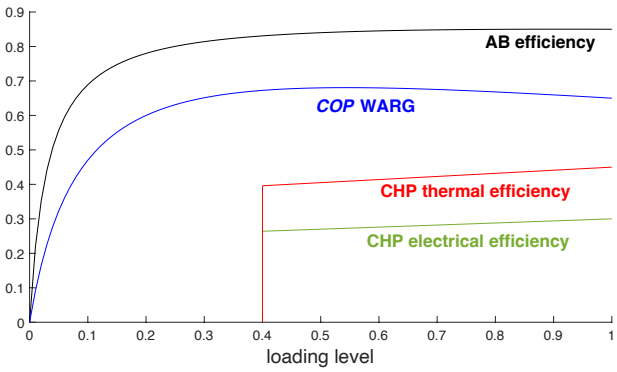


Fig. 3. Variable efficiencies and *COP* of the equipment.

Table II. Curve Fitting Coefficients

| ***W*,CHP** | ***Q*,CHP** | **AB** | **WARG** |
|---|---|---|---|
| $c_{W,0} = 0.24$<br>$c_{W,1} = 0.06$<br>$c_{W,2} = 0$ | $c_{Q,0} = 0.36$<br>$c_{Q,1} = 0.09$<br>$c_{Q,2} = 0$ | $\upsilon_0 = 0.0347$<br>$\upsilon_1 = 0.1005$<br>$\upsilon_2 = 0.0413$ | $\varsigma_0 = 0.0987$<br>$\varsigma_1 = 0.1067$<br>$\varsigma_2 = 0.3331$ |

The analysis is divided into two representative days, for the winter period and for the summer period, respectively. In the winter period the EHP operates in heating mode, while in the summer period the EHP operates in cooling mode. The electrical, heating and cooling demand is shown in Fig. 4 for the two periods. The electricity and fuel prices are reported in Fig. 5, with indications in monetary units (m.u.).

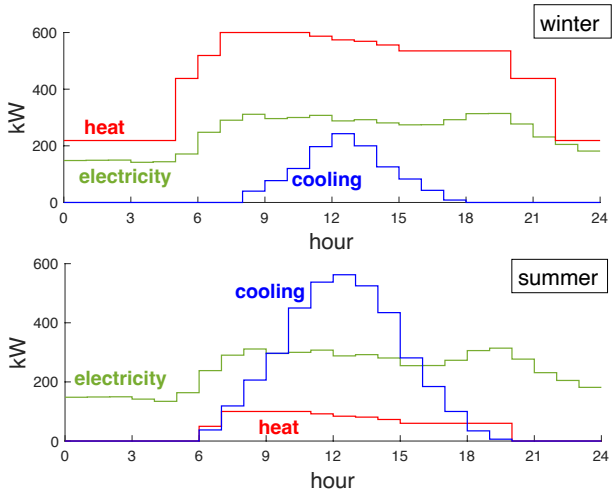


Fig. 4. Electrical, heating and cooling demand in the winter and summer periods.

### B. Hourly Optimization Results

The optimization is carried out by considering the minimum cost (13) and the constraints indicated in Section II.C. The tolerance for the stop criterion is set to $10^{-5}$.

Fig. 6 reports the number of iterations of the optimization with variable efficiencies and *COP*. In the summer cases, there are some hours in which the heat demand and the cooling demand are null. In these cases, there is no need for running the optimization, as the CHP is switched off and the electrical demand is served from the EDS. For this reason, the number of iterations reported is null and the cost has a unique value, which depends on the electricity bought from the EDS and on the price coefficient $\rho_{W,\text{buy}}$.

In the winter case, the number of iterations is generally low (from 2 to 5). In the summer case, the number of iterations is higher, due to the larger interaction among the components, in particular, to serve the cooling load.

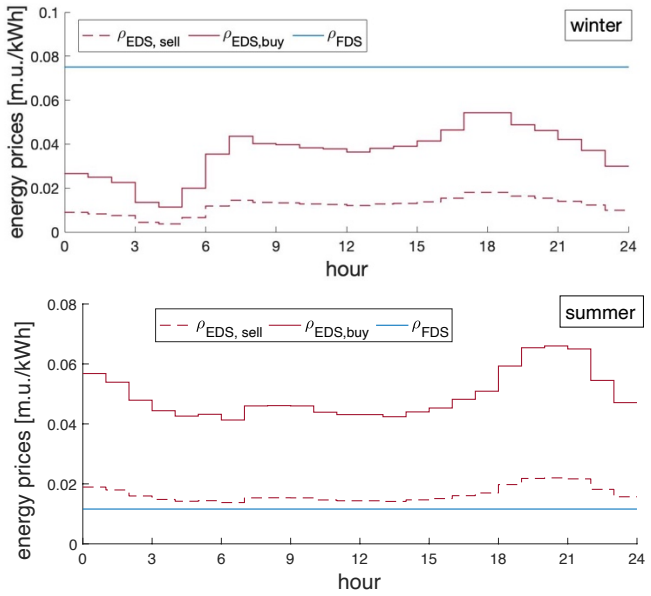


Fig. 5. Energy prices in the winter and summer periods.

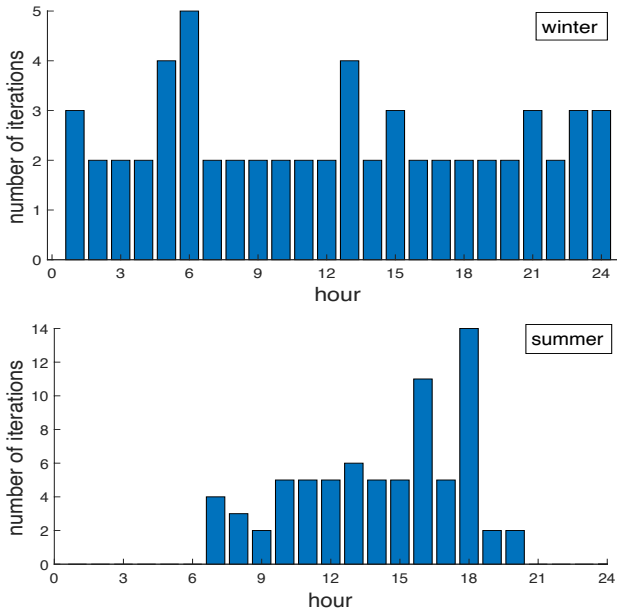


Fig. 6. Number of iterations for the optimization with variable efficiencies and *COP*.

However, the increased number of iterations does not imply large fluctuations in the results. For example, considering the summer case with the higher number of iterations (hour 18, with 14 iterations to converge), Fig. 7 shows that, with the strict tolerance used in the stop criterion, the variations in the CHP and WARG outputs are very low, as there is only a slight fluctuation in these outputs (detailed for the CHP electrical output in the zoom of Fig. 8). As such, the proposed approach provides the solution by using the non-linear representation of the efficiencies and *COP*, without the need of resorting to approximate representations (such as piecewise linearizations) of the non-linear parameters in function of the loading level.

Fig. 9 shows the costs obtained from the cases with constant and variable efficiencies and *COP*. In the winter case, the cost with variable efficiencies and *COP* is generally slightly higher than the cost obtained with constant values.

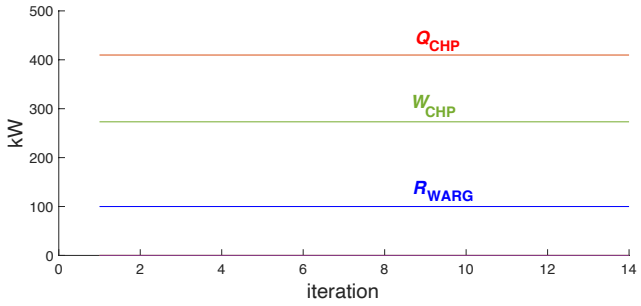


Fig. 7. Variations in the CHP and WARG output during the iterative process in the summer case at hour 18.

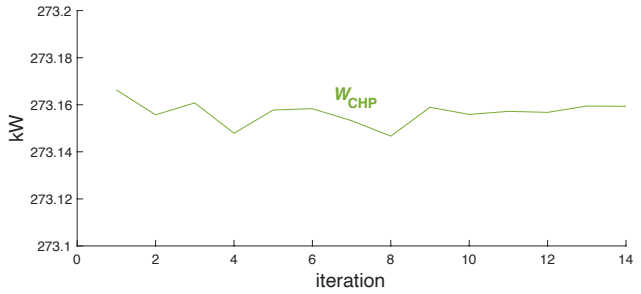


Fig. 8. Zoom of the variations in the CHP electrical output during the iterative process in the summer case at hour 18.

This happens because there is a prevailing usage of the equipment to serve heat, in which the efficiency at partial load is lower. In the summer case, there are a few hours in the central part of the day in which the cost with variable efficiencies and *COP* is slightly lower than the cost with constant values, mainly due to the usage of the WARG at partial loading corresponding to higher *COP* with respect to the rated *COP*.

From the results obtained by using a MacBook Pro with 2.3 GHz Intel Core i9 8 core processor, the computation time ratio is $\tau_r \cong 3$ for the winter case and $\tau_r \cong 3.8$ for the summer case. The average computation time per iteration is $\tau_a \cong 0.12$ s for the winter case and $\tau_a \cong 0.15$ s for the summer case.

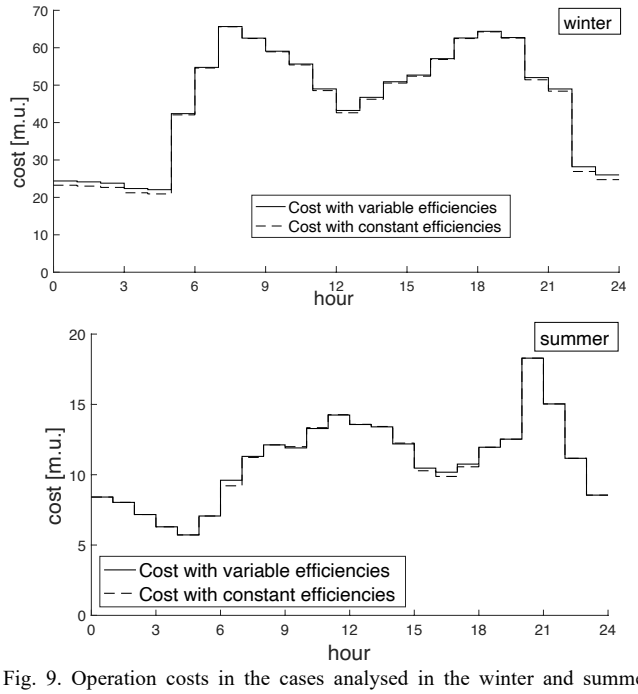


Fig. 9. Operation costs in the cases analysed in the winter and summer periods with constant and variable efficiencies and *COP*.

### C. Example of Optimization Results for a Selected Hour

The hourly average power resulting from the optimization with constant and variable efficiencies and *COP* are shown in Fig. 10 for the winter case study at hour 11:00, and in Fig. 11 for the summer case study at hour 11:00. In both cases, the solutions with constant and variable efficiencies and *COP* are consistent and slightly different only depending on the performance of the equipment used.

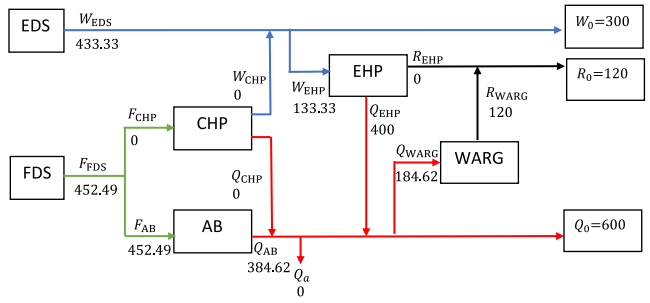


a) constant efficiencies and *COP* (values in kW)

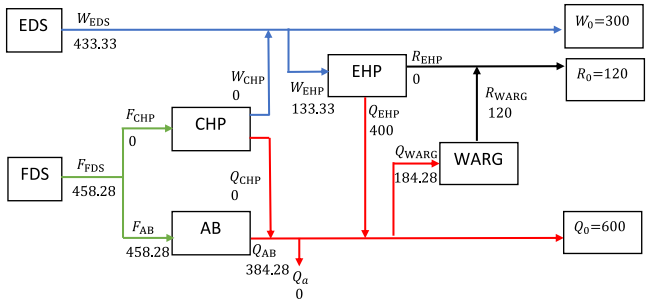


b) variable efficiencies and *COP* (values in kW)

Fig. 10. Optimal solutions at hour 11:00 in the winter case study with constant and variable efficiencies and *COP*.

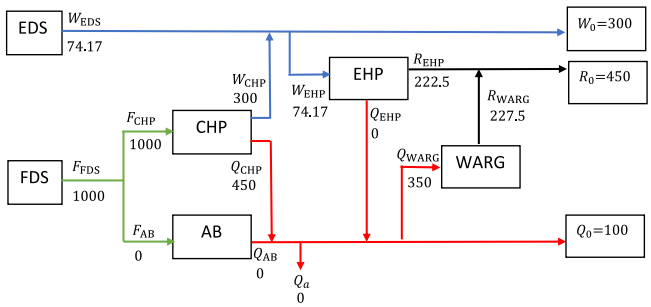


a) constant efficiencies and *COP* (values in kW)

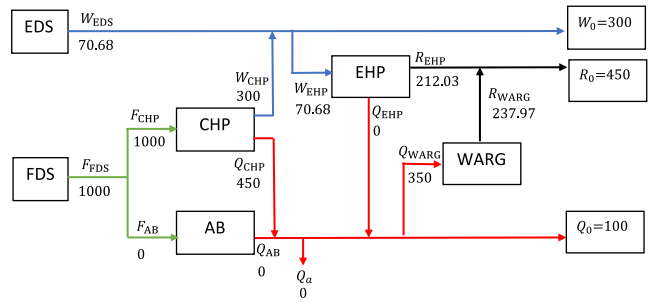


b) variable efficiencies and *COP* (values in kW)

Fig. 11. Optimal solutions at hour 11:00 in the summer case study with constant and variable efficiencies and *COP*.

In the winter case, the CHP is switched off. The EHP operates at its maximum capacity and has constant efficiency, so that there is no variation on the electrical side. The only difference appears on the AB, with lower efficiency at partial loading with respect to the rated efficiencies, while the WARG has a slightly higher *COP* with respect to its rated *COP*. As a result, at variable efficiencies and *COP* the fuel input is higher and increases the total operation cost.

In the summer case, in both solutions the CHP operates at its maximum loading and the AB is not used, so that the fuel input is the same. With variable efficiencies and *COP*, the WARG has a higher *COP* with respect to its rated *COP*, so that less cooling output is requested from the EHP. Thereby, the electricity bought from the EDS is lower, and the total operation cost is lower than with constant efficiency and *COP*.

## V. Conclusions

This paper has presented an extended optimization procedure that iterates the optimization model with linear constraints to provide the optimal solution when the efficiencies and *COP*s of the MES equipment are variable with the loading level. The extended optimization procedure has been used to define optimal operational strategies in different periods, represented as a winter case and a summer case with different contributions of the electricity, heat and cooling patterns, and different energy prices. The results show that the proposed optimization procedure is viable and can reach the optimal solution after a limited number of iterations also with strict tolerance for the stop criterion.

Further work is in progress to apply the extended optimization procedure for identifying the MES flexibility in the optimal MES operating conditions, considering the construction of the feasibility regions [11] and of the MES flexibility maps [12], for different types of multi-energy energy systems, districts and communities.

## References


[1] P. Mancarella, "MES (multi-energy systems): an overview of concepts and evaluation models," *Energy*, vol. 65, pp. 1–17, 2014.

[2] E.A. Martinez Cesena, E. Loukarakis, N. Good, and P Mancarella, "Integrated electricity-heat-gas systems: techno-economic modeling, optimization, and application to multienergy districts," *Proceedings of the IEEE*, vol. 108 (9), pp. 1392–1410, 2020.

[3] M. Geidl, G. Koeppel, P. Favre-Perrod, B. Klockl, G. Andersson, and K. Frohlich, "Energy hubs for the future," *IEEE Power & Energy*, vol. 5, no. 1, pp. 24–30, 2007.

[4] G. Chicco and P. Mancarella, "Matrix modelling of small-scale trigeneration systems and application to operational optimization," *Energy*, vol. 34, no. 3, pp. 261–273, 2009.

[5] Y. Wang, J. Cheng, N. Zhang, and C. Kang, "Automatic and linearized modeling of energy hub and its flexibility analysis," *Applied Energy*, vol. 211, pp. 705–714, 2018.

[6] Y. Wang, N. Zhang, C. Kang, D.S. Kirschen, J. Yang, and Q. Xia, "Standardized matrix modeling of multiple energy systems," *IEEE Trans. on Smart Grid*, vol. 10 (1), pp. 257–270, 2019.

[7] M.R. Almassalkhi and A. Towle, "Enabling city-scale multi-energy optimal dispatch with energy hubs," *2016 Power Systems Computation Conference (PSCC)*, Genoa, Italy, 2016, pp. 1-7.

[8] W. Huang, N. Zhang, Y. Wang, T. Capuder, I. Kuzle, C. Kang, "Matrix modeling of energy hub with variable energy efficiencies," *Electrical Power and Energy Systems*, vol. 119, art. 105876, 2020.

[9] R. Siohansi and A.J. Conejo, *Optimization in Engineering: Models and Algorithms*, Springer, 2017.

[10] P. Mancarella and G. Chicco, *Distributed multi-generation systems: energy models and analyses*, Nova Science Publishers, New York, 2009.

[11] J. Hinker, H. Knappe, and J.M.A. Myrzik, "Precise assessment of technically feasible power vector interactions for arbitrary controllable multi energy systems," *IEEE Trans. Smart Grid*, vol. 10, no. 1, pp. 1146-1155, 2019.

[12] G. Chicco, S. Riaz, A. Mazza, and P. Mancarella, "Flexibility from Distributed Multienergy Systems," *Proc. IEEE*, vol. 108, no. 9, pp. 1496-1517, 2020.